

PAPER • OPEN ACCESS

Investigation on the digital image correlation and charge trap characteristics of Al/epoxy nanocomposites

To cite this article: Naresh Chillu *et al* 2020 *Mater. Res. Express* 7 025035

View the [article online](#) for updates and enhancements.



The Electrochemical Society
Advancing solid state & electrochemical science & technology
2021 Virtual Education

Fundamentals of Electrochemistry:
Basic Theory and Kinetic Methods
Instructed by: **Dr. James Noël**
Sun, Sept 19 & Mon, Sept 20 at 12h–15h ET

Register early and save!





PAPER

Investigation on the digital image correlation and charge trap characteristics of Al/epoxy nanocomposites

OPEN ACCESS

RECEIVED

20 October 2019

REVISED

20 November 2019

ACCEPTED FOR PUBLICATION

4 December 2019

PUBLISHED

17 February 2020

Naresh Chillu¹ , R Jayaganthan² , R Velmurugan³ and R Sarathi¹ ¹ Department of Electrical Engineering, Indian Institute of Technology Madras, Chennai 600 036, India² Department of Engineering Design, Indian Institute of Technology Madras, Chennai 600 036, India³ Department of Aerospace Engineering, Indian Institute of Technology Madras, Chennai 600 036, IndiaE-mail: rsarathi@iitm.ac.in**Keywords:** nanocomposites, digital image correlation, charge trap, tensile strength

Original content from this work may be used under the terms of the [Creative Commons Attribution 3.0 licence](https://creativecommons.org/licenses/by/4.0/).

Any further distribution of this work must maintain attribution to the author(s) and the title of the work, journal citation and DOI.

**Abstract**

The influence of nanofiller on the tensile and surface charge properties of Al/Epoxy nanocomposite materials is investigated with respect to their structural composition. The formation of conductive network nearing the percolation limit with the addition of nanofiller has strongly influenced the mechanical and electrical characteristics of nanocomposites. The digital image correlation technique is employed to acquire the strain variation at the distinct locations on the tensile specimen. The load-displacement, as well as shape deformation, were analysed for the various nano filled composites. The improved tensile characteristics were achieved up to certain wt% of filler addition, beyond which the load and time required for the material fracture were reduced drastically. Likewise, the addition of filler up to 5 wt% has shown the improved charge decay characteristics viz. quicker charge decay and enhancement in shallow energy states under the applied DC voltage. The direct analogy in mechanical and electrical characteristics was formulated in terms of structural composition (defects, additives and filler) of respective materials.

1. Introduction

Nanostructuration provides the high aspect ratio and specific surface area to improve the thermal, mechanical and electrical properties of nanocomposite material [1, 2]. They have the advantage of low cost, lightweight, ease of processing, increased modulus and strength, thermal stability, erosion resistance, good electrical insulation characteristics and high breakdown strength over the polymer matrix [3–5]. Lower addition of filler to the base polymer matrix result in uneven dispersion, in contrast, higher concentration leads to agglomerations which deteriorate the load-bearing capability of the overall material [6]. It is an utmost concern for the researchers to identify the optimised filler concentration which ensures the efficient filler dispersion in the polymer matrix for enhancing the overall properties of the material.

The mechanical–electrical analogies proved that certain mechanical problems would be solved easily in the electrical domain. For example, the piezoelectric effect which links the crystal resonator having mass, spring and damper elements to the equivalent electrical systems with a capacitor, inductor and resistor respectively in the direct analogy. The desired properties viz. the resonant frequency which is a function of electrical components is modelled by adjusting the structural properties of the crystal in the mechanical domain [7]. However, understanding the correlation between electromechanical properties is an open subject for the researchers worldwide.

Earlier studies revealed that the improvement in tensile behaviour of epoxy nanocomposite materials merely depends on the efficient filler dispersion and the interfacial adhesion between filler and the matrix [8–10]. The polymer nanocomposite materials with conductive fillers find their applications include embedded capacitance material (ECM), high energy density capacitors, and electromagnetic interference (EMI) shielding material in electronic circuits [5]. Also, these metallic filled nanocomposite materials exhibit excellent dielectric characteristics below the percolation threshold characteristics viz. high breakdown strength, better space charge

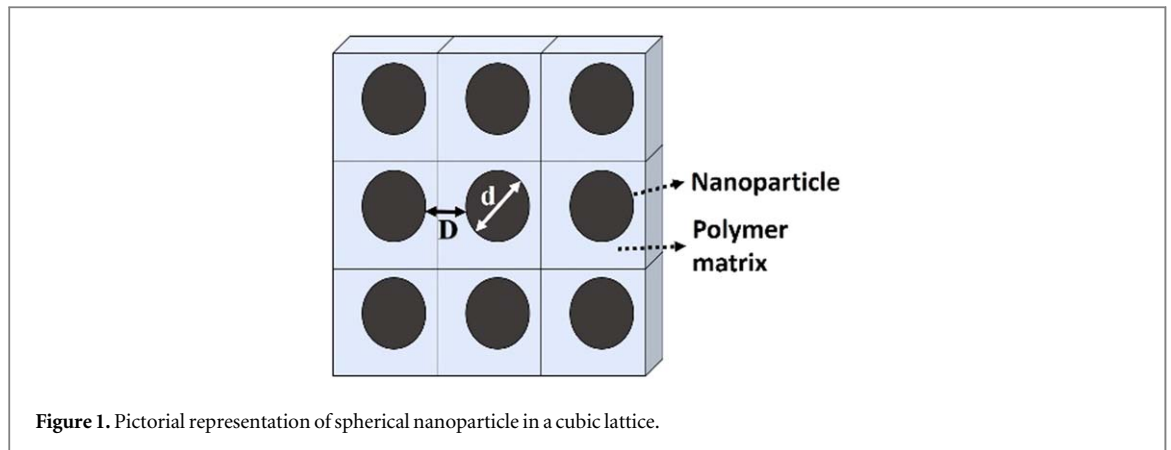


Figure 1. Pictorial representation of spherical nanoparticle in a cubic lattice.

behaviour [11, 12]. Aluminium filled nanocomposite materials have shown a better thermal stability, heat dissipation and thermal conductivity over the base material [13, 14]. Anithambigai *et al* have investigated the thermal characteristics of an LED employing metal aluminium filled polymer nanocomposites as a thermal interface material for an improved heat dissipation properties [15]. Bello *et al* have investigated the influence of the addition of nano and micro aluminium fillers on the tensile behaviour and shown that the nano filled materials have exhibited improved tensile strength over micro composites [16]. Since the inherent defects in the material initiate the fractures under mechanical loading, it is essential to understand the variation in the strain at distinct locations on the specimen specifically at the fracture points, rather just examining the cumulative strain experienced by the specimen [17, 18]. On the other hand, the surface of the material is mostly exposed to the stresses during the power apparatus operation. The localised surface traps resulting from the material composition defines the magnitude of charge transport through the material. Under the normal operating condition, the inherent defective states in the insulating material accumulate the charge within the bulk volume initiated from the surface trap sites, causing the local electric field enhancement, leading to internal damage locally and over a period of time, a catastrophic failure can occur [19–21]. Therefore, it is essential to design the materials which are capable of mitigating the enhancement in the electric field during the power apparatus operation by the least charge accumulation and instantaneous charge decay upon removal of the field conditions [22, 23]. The analysis of such study with epoxy nanocomposites reinforced with conducting filler is scarce in the literature.

Having known these differences, the present study is carried out to investigate the correlation between strain variation and surface charge decay characteristics of different epoxy nanocomposite (with nano aluminium as filler) materials and discuss the correlation in respect to the structural properties (filler, additives and defects) of the nanocomposite material. Methodical experimental studies were carried out to understand the following important aspects, such as (a) investigating the tensile behaviour, as well as, the strain variation at distinct locations on the specimen using digital image correlation (DIC) technique, well-known method for studying full-field displacement and surface strain variation for different nanocomposite materials, and (b) inspecting the surface charge decay characteristics of epoxy nano aluminium composites viz. potential decay and trap distribution properties under the DC voltage for positive and negative polarity.

2. Experimental studies

2.1. Selection of filler size and optimised weight fraction

In the present study, Al nanoparticles with an average particle size of 40 nm were chosen. The percolation threshold is the upper limit on the addition of nanoparticles to the polymer matrix, upon exceeding which causes the drastic increment in the electrical conductivity of the composite material.

Considering the spherical nanoparticle with diameter, d is dispersed in a cubical lattice of polymer matrix as shown in figure 1, the inter filler distance, D between the two neighboring nanoparticles as a function of filler concentration (wt%) is calculated through the following equation (1) [24],

$$D = \left\langle \left\{ \frac{\pi}{6} \left(\frac{\rho_n}{\rho_m} \right) \frac{100}{\text{wt \%}} \left[1 - \frac{\text{wt \%}}{100} \left(1 - \frac{\rho_m}{\rho_n} \right) \right] \right\}^{\frac{1}{3}} - 1 \right\rangle * d \quad (1)$$

Table 1. Variation in inter filler distance as a function of filler concentration.

wt%	D (nm)						
1	157.4	7	62.0	13	42.0	19	31.3
2	116.4	8	57.4	14	39.8	20	30.0
3	96.3	9	53.4	15	37.8	21	28.7
4	83.6	10	50.0	16	36.0	22	27.6
5	74.5	11	47.0	17	34.4	23	26.5
6	67.6	12	44.4	18	32.8	24	25.6

where ρ_n and ρ_m are specific gravities of Al nanofiller and the polymer matrix ($\rho_m = 1.17$ and $\rho_n = 2.7$), respectively. Intuitively, increased addition of nanoparticles in a polymer matrix reduces the inter filler distance. The inter filler distance calculated from equation (1) at different filler concentrations is tabulated in table 1.

It is clear from table 1 that the lower filler concentration result in maximum inter filler distance, indicating the uneven dispersion of nanoparticles. On the other hand, higher filler concentration results in the lower interparticle distance implying the overlapping of nanoparticles and hence the formation of the conductive network. Whereas the uniform dispersion is possible provided the inter filler distance, D is equal to the diameter of the nanoparticle, d . From table 1 it can be noticed that the diameter of nanoparticle (40 nm) and inter filler distance (39.8 nm) are almost equal at the filler concentration of 14 wt% [24–26]. In general, nanoparticle agglomerations and non-uniformity in filler matrix dispersion impose an upper limit on the practical percolation value. Hence, the actual threshold limit is lower than the theoretically calculated value. For the experimental studies, composite materials having aluminium nanofiller loadings with 0, 1, 5 and 10 wt%, respectively are prepared in the present study.

2.2. Materials and method of sample preparation

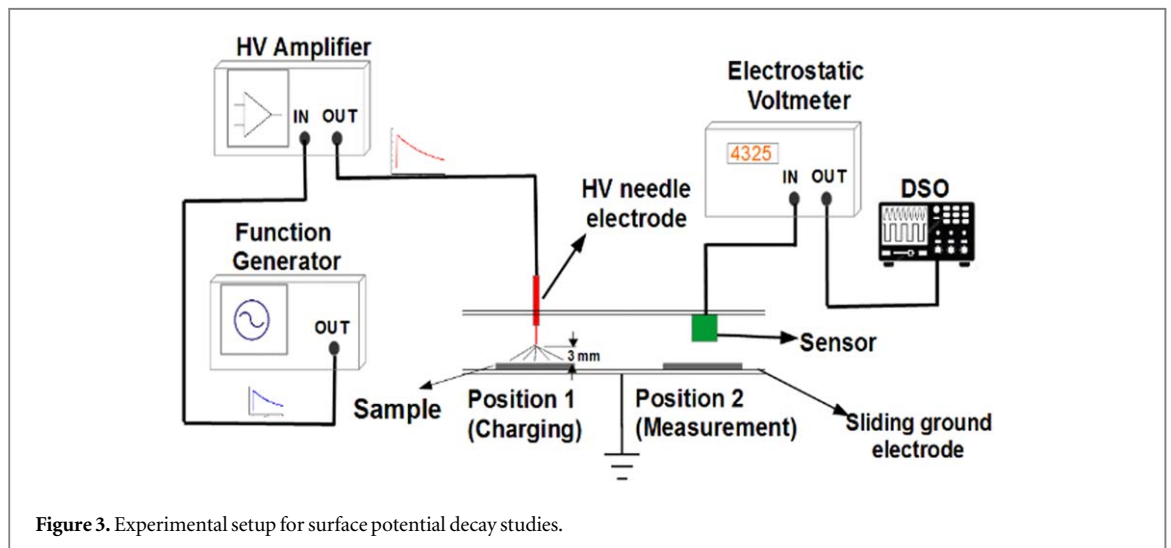
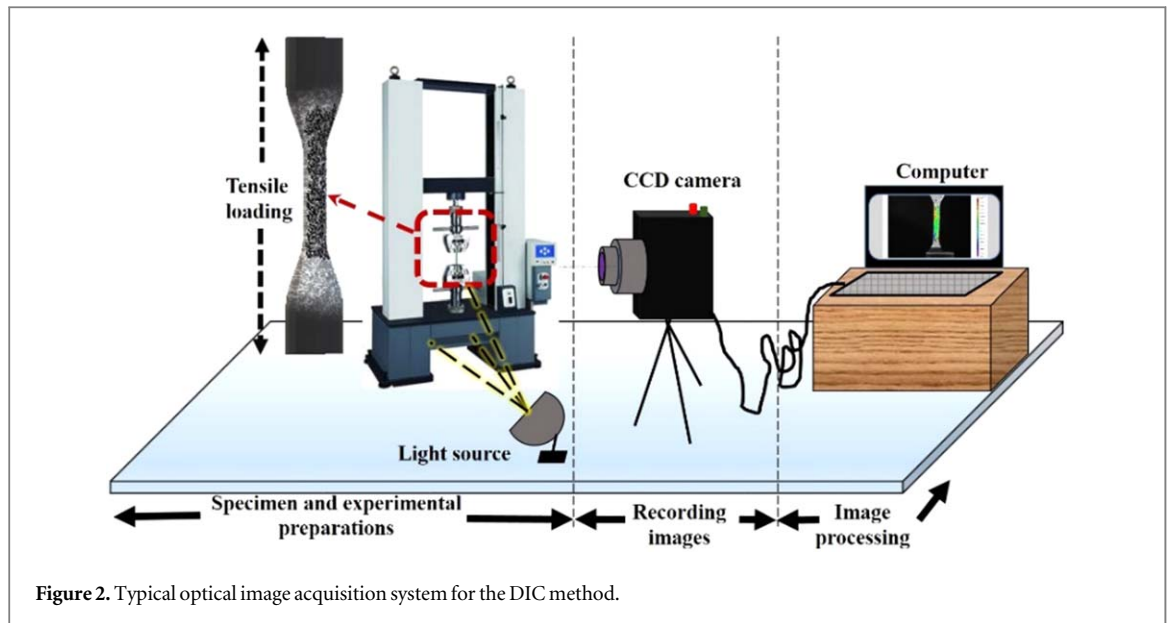
The materials used in the preparation process are, the Bisphenol-A epoxy resin (CY205) as a base polymer matrix, Tri-ethylene tetra-amine (TETA) hardener as a curing agent and self-passivated spherical aluminium nanoparticles of 99.9% purity with an average particle size of 40 nm (supplied by Hongwu International Group Ltd, Hong Kong) as a filler material. The nanocomposite materials were fabricated by adding different weight percentage of nanofillers to the base epoxy matrix, adopting the following preparation procedure. At the initial stage, the required quantity of nano aluminium powder was heated at 110 °C, for 3 h to remove the traces of moisture in it. Next, the heated nanofiller was mixed with ethanol and sonicated for 1 h. Subsequently, the nanoparticle dispersed ethanol was mixed with epoxy resin by shear mixing process for 6 h. At the later stage, the high frequency sonication process (at 20 kHz) was carried out, for two h, by maintaining the sample temperature at 40 °C in ice filled water bath. At the final stage, prior to the addition of hardener for curing, the mixture was kept in an oven for allowing the excess ethanol to evaporate from the mixture. At the sixth stage, the required quantity of hardener was added to the nanoparticle dispersed epoxy mixture and mixed thoroughly till uniform dispersion was achieved. On degassing, the mixture was poured into a mould in required dimensions for various tests.

2.3. Mechanical characterisation

To investigate the filler effect to resist breakage under applied stress, the prepared samples are conventionally tested with universal Testing Machine of 20 kN loading capacity with a displacement rate of 2 mm min⁻¹ at the room temperature. In this study, tensile specimens were prepared according to ASTM D-638 (Type IV) standard procedure in the dumbbell shape with the dimensions 115 × 6 × 3 mm and 25 mm gauge length. For the correctness and reliability of results, tests were carried out on 4 samples with the same concentration and averaged.

Digital image correlation is an efficient image-based technique for shape, field displacement and deformation measurements at distinct locations over the surface of the specimen under test [27, 28]. The typical experimental setup illustrating the schematic of DIC method is shown in figure 2. The following steps are implemented successively to obtain the desired displacements and strain information: specimen and experimental preparation, recording the images and post-image processing.

Speckle pattern on the surface of the specimen act as a carrier of deformation during the tensile loading. The artificial speckle pattern is performed on the specimen surface since the surface texture of prepared nanocomposites are not providing ample intensity variations. The specimen is speckled with black dots using a permanent marker pen on white paint over the sample surface. To map the in-plane deformation during tensile loading, utmost care was taken while performing speckle pattern on the sample surface, viz. (a) showing non-repetitive/ random pattern, (b) marked pattern adhere tightly to the specimen surface and (c) providing high-



intensity levels for better capturing through CCD camera. Under the tensile loading, the displacement in the speckle pattern is recorded continuously by a Grasshopper CCD camera (with Sony ICX625 2/3' sensor) of 5.0 MP with a maximum resolution of 2448×2048 pixels placed at 50 cm in front of the universal testing machine. The lens used with the camera is of Canon has a fixed focal length of 50 mm. LED light source was utilized to brighten the speckle pattern on the sample surface while capturing the images during the loading. The captured images are acquired through the Grasshopper GRAS-50S5 IEEE-1394b graphical user interface and subsequently recorded in the computer. The VIC-2D software provided by Correlated Solutions, Inc. was employed to post-process and analyses the acquired digital images and perform the correlation-based matching algorithm. The optimized subset, step size and strain filter of 29, 5 and 21 respectively 5 are used while performing the DIC analysis. For uniform speckle pattern and unvaried experimental conditions for a given specimen, the localized virtual strain gauge is determined by multiplying step size and strain filter. Thus, it provides in-plane full-field displacements and strains by comparing the digital images of the specimen surface in the reference and deformed states respectively.

2.4. Surface potential measurements under DC voltage:

The experimental setup as shown in figure 3 is employed to investigate the surface potential decay characteristics for the nanocomposites, for the positive and negative polarity of the applied voltage. The experimental setup used in carrying out the surface potential measurements is a widely adopted non-contact method of charging the test specimen, having the provision to test the insulating materials for different voltage profiles [12, 19, 29] and at different temperature ranges [30].

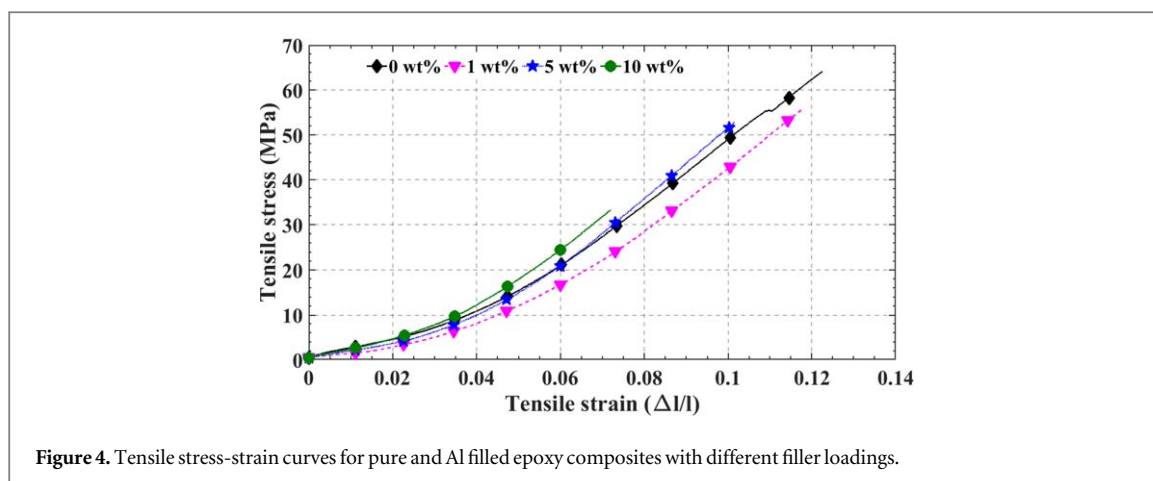


Figure 4. Tensile stress-strain curves for pure and Al filled epoxy composites with different filler loadings.

Table 2. Variation of Tensile properties of Al/Epoxy nanocomposites.

wt%	Load at maximum tensile stress (N)	Youngs modulus, E (MPa)	Ultimate tensile strength, S_u (MPa)
0	1660	731.0	64.0
1	1053	748.3	55.7
5	1146	786.7	52.8
10	817	729.1	33.3

The needle plane configuration is used for charging the specimen. The specimen is placed in between the top needle electrode (tip radius of 0.3 mm) and the bottom ground plane electrode (sliding aluminium sheet). The high voltage amplifier generates the required voltage, with its input from the function generator. The configuration is used to inject the charges over the specimen which is located at position 1 for 3 min 3 mm space is maintained between the sample surface and the tip of high voltage electrode, throughout the experiment. After 3 min of charging, the sample is immediately brought under position 2 where the potential remain on the surface of the sample is measured under isothermal conditions through an electrostatic voltmeter (Trek model 341B) and subsequently data is recorded continuously in the DSO. In the present study, the surface potential decay measurements are conducted for positive and negative polarities of 10 kV DC voltage.

3. Results and discussion

3.1. Mechanical characterisation

Figure 4 shows the variation in tensile stress versus strain for pure epoxy and Al-epoxy composites with different filler loadings from 1 to 10 wt%. It is observed from figure 4 that an instant drop in the stress-strain curves, as soon as the material underwent the maximum load (ultimate tensile strength, S_u) point indicate the inherent brittle nature of composites. Also, the reduction in the strain at fracture point of samples and improving the stiffness of nanocomposites are observed over the pure epoxy material. As presented in table 2, it can be seen that Young's modulus which represents the stiffness of material, found higher for the nanocomposites with filler concentration and maximum for the material with 5 wt%. Likewise, the load required to cause fracture and the maximum stress undergone by the material (S_u) are low for the nanocomposite materials in comparison with the pure epoxy. Shape, filler dispersion and interfacial adhesion to the epoxy matrix are the crucial deciding factors for the mechanical characterization. As filler percentage is increased, particles get aggregated easily due to high specific surface area and stronger Van Der Waals forces between adjacent particles [8]. Further, filler packing density and non-uniform dispersion at higher filler concentrations create voids and weaken the bonding between filler and matrix which results in ineffective load transfer between matrix and filler, thereby fractures easily at lower loads [31]. Though the shape was same in all the samples, strong interfacial adhesion with the addition of nanofiller till 5 wt% manifesting that an efficient load transfer between matrix and filler, and hence improving Young's modulus of the nanocomposite materials. On the other hand, inefficient filler dispersion resulted from increased nanofiller concentration leads to the formation of agglomerations which further deteriorates the load-bearing capability of nanocomposite materials above 5 wt%.

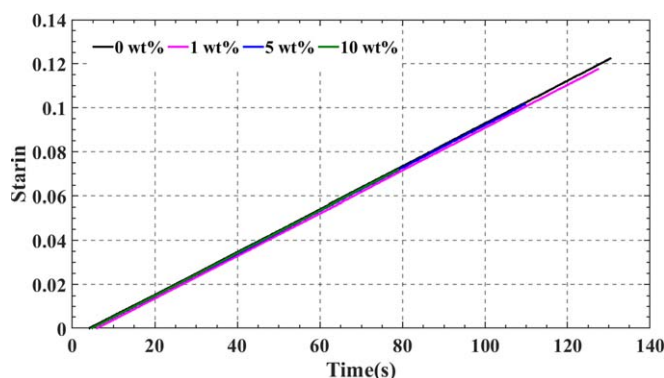


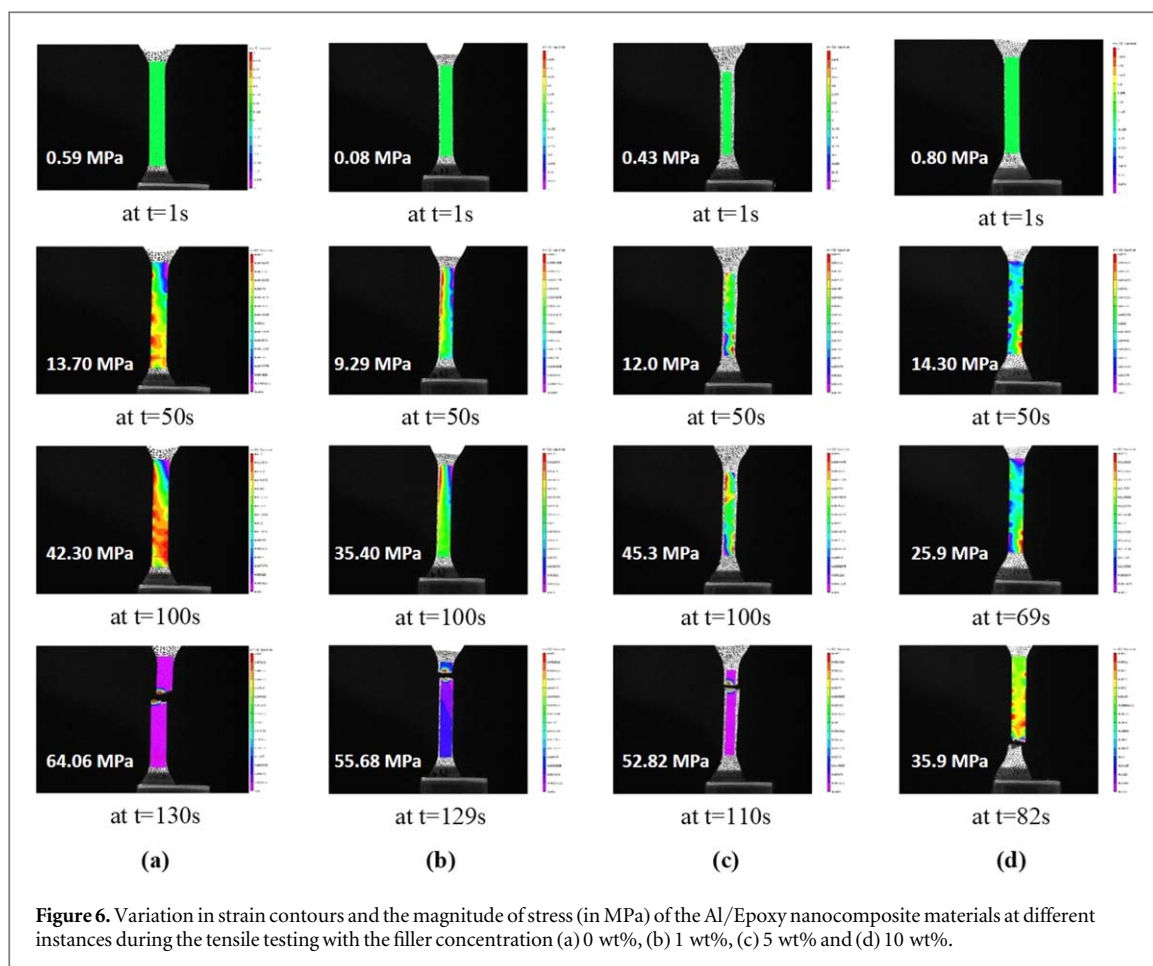
Figure 5. Variation in the tensile strain as a function of time in Al/Epoxy nanocomposites.

The cumulative strain distribution in the specimen with respect to time during the testing is shown in figure 5 for the nanocomposite materials. It can be noticed from figure 5 that the strain experienced by the nanocomposite materials is reduced with the addition of filler. Also, the time taken for the breakage under uniform load conditions is reduced and it is sluggish till the addition of filler up to 5 wt%, whereas it is very less for the specimen above 5 wt% to initiate the breakage. The possible reason could be the reduction in inter filler distance between adjacent nanoparticles in the polymer matrix result in the agglomerations which further weakens the bonding between filler and matrix and therefore result in an ineffective load transfer between matrix and filler.

The DIC analysis was carried out on Al/Epoxy polymer nanocomposite materials to understand the influence of filler on the mechanical (tensile) behaviour. Unlike the conventional tensile testing, DIC measures the strain deformation at distinct locations over the surface of the specimen and provides the strain contours when the specimen is subjected to the tensile load [27, 32]. Figures 6(a)–(d) shows the variation in strain contours of the Al/Epoxy nanocomposite materials at different instances during the tensile test for the different nanofiller concentrations. The duration of the experimentation time is same for the tensile testing performed through conventional and DIC method. The stress (in MPa) measured at a particular instant during the conventional testing is matched with DIC image taken at the same instant while performing the post image processing, and it is represented in the vicinity of the image as shown in figure 6. The speckle pattern present in the reference image (at $t = 1$ s) is continuously compared with the deformed images ($t > 1$ s) and therefore the correlation between the corresponding images yields the plot contour of the strains in a particular specimen. It can be observed from figures 6(a)–(d) that the deformation field is concentrated slowly near the failure region over a period of time during the testing. Also, the strain field presented in the fourth row of figures 6(a)–(d) shows the failure of the sample at different locations under the tensile loading which can be attributed to the existence of high-stress concentration areas. The red colour in the legend of the strain contour diagram corresponds to maximum strain values while the purple colour corresponds to the minimum. The strain analysis generally quantifies the amount of deformation experienced by the test specimen which further classifies ductility or brittleness upon the application of tensile load.

It is well known that the strain experienced by the specimen at distinct locations is different and therefore the strain along the elongation (ϵ_{yy}) direction is analyzed by choosing the various locations on the surface of the sample. The positions on the specimen are selected so that the maximum, minimum and medium strain regions are covered. The procedure for selecting the distinct locations and their corresponding strain along the y -direction as a function of time for different nanocomposite materials is shown in (i) and (ii) of figures 7(a)–(d) respectively. The time indicated in the strain contour diagram corresponds to the instant at which DIC analysis is being carried out, which essentially represents the image acquired from the third row of figure 6. Location 3 corresponds to the maximum strain region where the material breakage is inevitable. It is observed that the elongation in tensile direction (ϵ_{yy}) is increased linearly with respect to time regardless of the filler and location of interest. For a given material, it can be noticed that the ϵ_{yy} is higher at the maximum strain region (Location 3 in the deformed image) then followed by the medium strain region (Location 2) and the minimum strain region (Location 1).

Further, the variation in the elongation in tensile direction at maximum strain region (Location 3) obtained from DIC analysis is plotted in figure 8 to understand the distribution of strain in nanocomposite materials and its dependence on the addition of nanofiller. A clear variation in the strain distribution resulted from DIC technique can be observed from figure 8 with respect to time for all the nanocomposite materials in contrast to the similar analysis carried out with the conventional testing represented in figure 5. In addition, the strain



experienced by the nanocomposites as well as the time taken for the breakage under uniform load conditions is reduced slightly till 5 wt%, whereas the rapid reduction in time taken for the breakage of the specimen is observed for the sample with 10 wt% nanofiller inclusion. The addition of nanoparticles yields the reduction in inter filler distance between adjacent nanoparticles in the polymer matrix, further result in the agglomerations which weaken the bonding between filler and matrix at higher concentrations and therefore result in an ineffective load transfer between matrix and filler. The similar variation is observed with the conventional tensile testing shown in figure 5, which indicates that the DIC method can detect the full-field shape, deformation, displacement and contour of strain measurements in the sample subjected under mechanical loading.

The elastic object experiences the deformation under the application of force on it. From a mechanical point of view, it is evident from the strain analysis for the Al/Epoxy nanocomposite materials that the addition of nanofiller reduces the time and load required to cause failure. The anticipated reason could be the addition of nanoparticles implies the reduction in inter filler distance between adjacent nanoparticles in the polymer matrix that results in the agglomerations which further weakens the bonding between filler and matrix at higher concentrations and therefore result in an ineffective load transfer between matrix and filler.

In the quest of finding correlation in the electrical domain, the effect on surface charge variation under the applied uniform voltage with the addition of nanoparticles to the polymer matrix is analyzed further. It has been shown that the aluminium nano particle-filled composite materials below the percolation threshold would essentially exhibit the dielectric characteristics [5, 25].

3.2. Surface potential decay studies

The localized states arising prominently from the structural and intentional impurities act as charge carrier traps, which strongly influence the charge transport characteristics in the material. For the present experimental electrode configuration and specimen thickness, the applied electric field is not high enough for the charge carriers to transport through the volume of the material. Thermal agitation due to collision of charges allows the injected charge carriers to accumulate on the surface trap sites during the corona charge injection. Thus, the accumulated charge at the surface states of the specimen is expected to decay by recombining with the ions of opposite sign in the surrounding ambience, rather transporting through the bulk, under the absence of applied

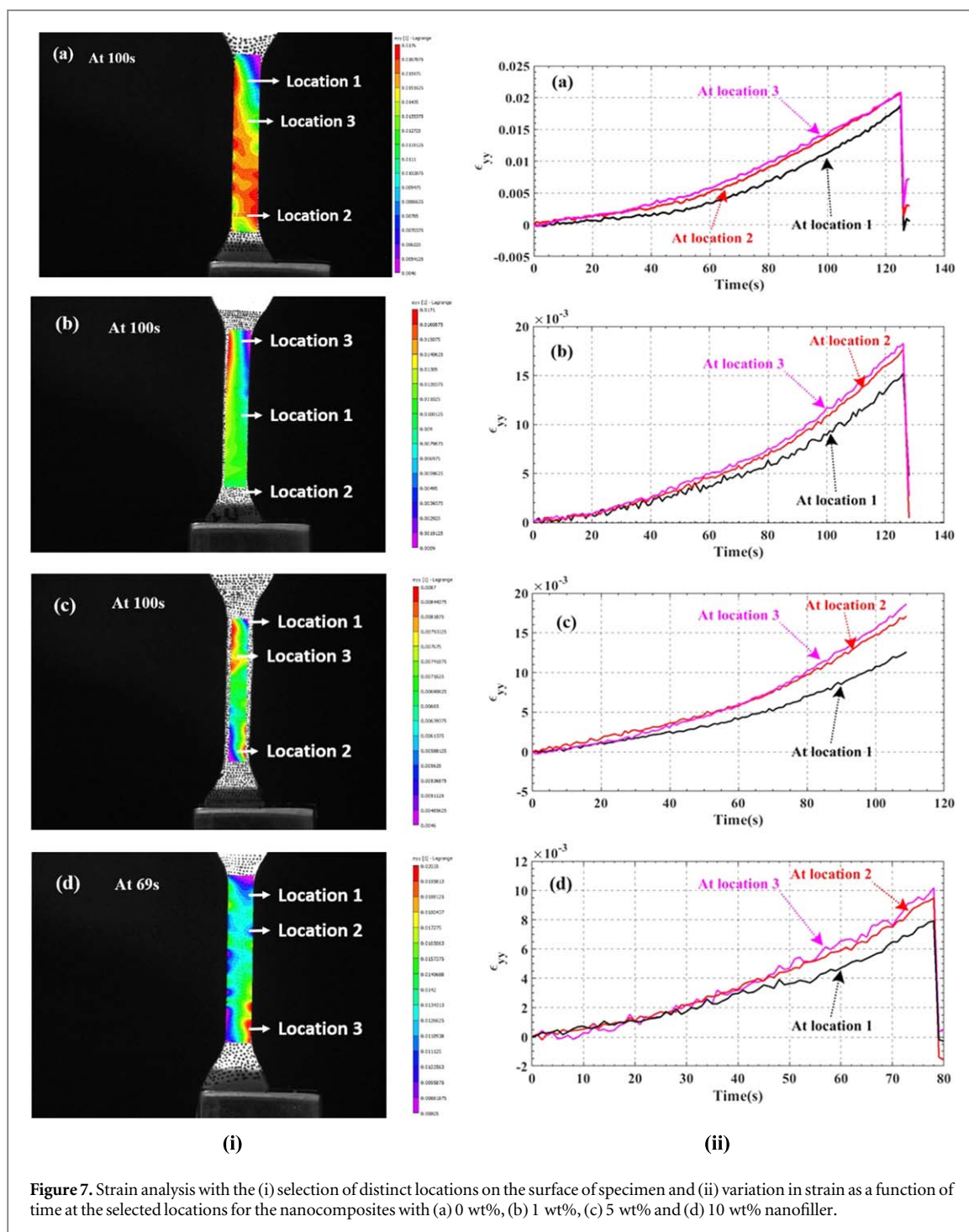


Figure 7. Strain analysis with the (i) selection of distinct locations on the surface of specimen and (ii) variation in strain as a function of time at the selected locations for the nanocomposites with (a) 0 wt%, (b) 1 wt%, (c) 5 wt% and (d) 10 wt% nanofiller.

voltage. Thus, the decay in surface potential measured through electrostatic voltmeter is directly related to decay of surface charge under the present experimental conditions.

The variation in the potential decay characteristics from the trapping sites on the surface of the different nanocomposite materials is plotted in figure 9 for the applied positive and negative DC voltage profiles. It is observed that the surface potential is decreasing exponentially regardless of the filler concentration and the applied polarity. The exponential decay in surface potential on the removal of charge injection from corona electrode is quantified mathematically as,

$$U(t) = U_0 e^{-\lambda t} \quad (2)$$

where U_0 is the initial potential and λ is the decay rate constant. Studies have shown that initial fast potential decay is attributed to detrapping of charges from shallow traps, and subsequent slower potential decay is ascribed to detrapping from deep traps [19]. Though the variation in magnitude of accumulated surface potential is insignificant for a given polarity, a significant variation can be noticed in the decay rate of the nanocomposite materials. The decay rate of the different nanocomposite materials under +DC and -DC is shown in table 3.

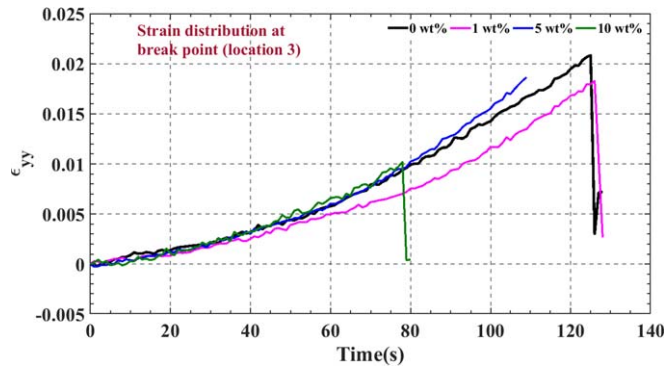


Figure 8. Variation in the elongation in y-direction at the maximum strain region for various Al/Epoxy nanocomposite materials.

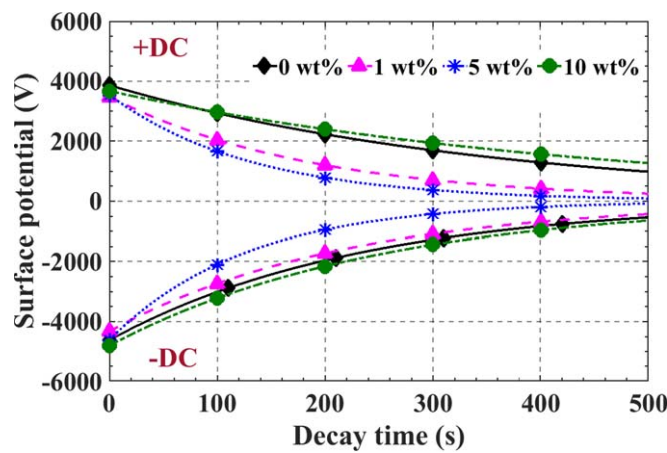


Figure 9. Surface potential decay plot for +DC and -DC input voltage.

Table 3. Trap parameters of Al/Epoxy nanocomposites under DC voltage.

Polarity wt%	Positive polarity		Negative polarity	
	Decay rate (s ⁻¹)	Trap centre (eV)	Decay rate (s ⁻¹)	Trap centre (eV)
0	0.0028	0.8664	0.0036	0.8550
1	0.0054	0.8492	0.0046	0.8532
5	0.0076	0.8402	0.0079	0.8392
10	0.0021	0.8730	0.0040	0.8567

Further, the density of trapped charge carriers $N(E)$ in a specimen at different energy levels (E) is analysed to acquire a better perspective of how strongly the injected charge carriers trapped in the localized surface states exist in the nanocomposite material [33]. The density of trapped charges ($N(E)$) at different energy levels (E) within the bulk of the material with the variation of trap depth (ΔE) [34, 35] is expressed by the following equation:

$$N(E) = \frac{4\epsilon_0\epsilon_r}{eL^2kT} \left| t \frac{dU}{dt} \right| \quad (3)$$

and the trap depth,

$$\Delta E = E_c - E_d = kT \ln(vt) \quad (4)$$

where ' L ' (in m) is the thickness of material, ' k ' (in J/K) is the Boltzmann constant, T (in K) is the thermodynamic temperature, E_c is the bottom of the transport state, and ' E_d ' is the demarcation energy level which separates the emptied and occupied states and v is the attempt to escape frequency, in order of 10^{12} s^{-1} . Trap depth is the

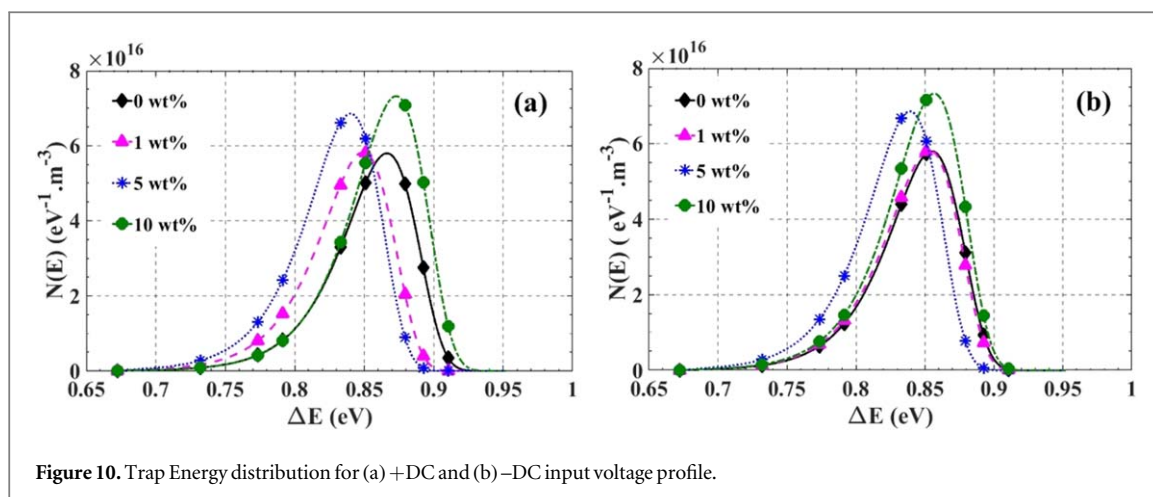


Figure 10. Trap Energy distribution for (a) +DC and (b) -DC input voltage profile.

amount of energy required for a charge carrier to get liberated from the localized trap site [20]. The trap depth at maximum energy density is treated as a trap centre [36]. Variation in trap centre for positive and negative polarities of the applied DC voltage profiles as a function of filler concentration is shown in figures 10(a) and (b).

It is observed that the trap distribution covers the range from 0.7 eV to 0.9 eV. Variation of trap centres with respect to the addition of filler and polarity of applied voltage profiles is shown in table 3. It is evident that the trap centre is reduced (left shift) for the nanocomposite materials slightly from 0 to 5 wt% of filler addition, beyond which the increment in the trap centre is noticed.

Addition of nanofiller to the epoxy matrix leads to the reduction in the inter-filler distance, contributing to the improvement in the carrier mobility for the materials up to 5 wt%. Considering the multi-core model, the charge carriers get detrapped from the shallow trap region (the loosely bounded layer) since it is low in density and occupies a large amount of free volume [24]. Whereas, further reduction in inter filler distance nearing the percolation threshold enhances the clusters of nanoparticles in the polymer matrix, leading to the migration of charge carriers at shallower traps to the deep trap states (through the second layer), for the nanocomposite material above 5 wt%. A considerable amount of energy is required for these charge carriers trapped in a cluster of localized states to get liberated and therefore the trap energy is increased for 10 wt% material. Thus, the reduction in trap centre is fundamentally related to faster decay characteristics of the material (up to 5 wt%), whereas, the increment in trap centre corresponds to the reduced decay rate of the material (10 wt%). The left shift in the trap centre is intuitively thought as the reduction in trap centre and it can be correlated with the increment in the decay rate of potential decay curves.

3.3. The electromechanical characteristics

The electromechanical behaviour is investigated in the present study for the epoxy nanocomposite materials fabricated with the incorporation of varying concentration of Al nanoparticles. The strain distribution analysis using DIC technique for the samples subjected to uniform mechanical loading conditions at the high stress concentrated regions result in the strain experienced by the nanocomposites as well as the time taken for the breakage under uniform load conditions is reduced invariantly till 5 wt%, whereas, the rapid reduction in strain and the time taken for the breakage of the specimen is observed for the sample with addition of 10 wt% nanofillers. Addition of nanoparticles causes the reduction in inter filler distance between adjacent nanoparticles in the polymer matrix, leading to the agglomerations which further weakens the bonding between filler and matrix at higher concentrations and therefore result in an ineffective load transfer between matrix and filler. Likewise, in a quest to investigate the equivalent electrical behaviour under uniform electrical loadings, the surface potential characteristics were analysed in contrast to the variation in surface strain analysis carried out through DIC technique under the mechanical loading. Availability of shallow energy states till optimum concentration (5 wt%) of nanoparticles allows the charge carriers to detrapp quickly. Whereas, the excessive addition of nanofiller diminishes the available inter filler distance, thereby the enhanced deep trap states result in the increased charge accumulation.

Interestingly, the resemblance in surface potential characteristics is devised with the surface strain variation under tensile loading as follows. The insignificant variation in the surface strain, as well as the time required for the breakage under the tensile loading up to 5 wt% of the material, is correlated to the increased surface potential decay rate as well as the reduced trap depth in the electrical domain. Thus, the optimized surface strain distribution resulted from the efficient load transfer between the matrix and filler from DIC analysis corresponds to the existence of shallow energy states in providing faster surface potential decay characteristics.

On the other hand, the drastic reduction in surface strain, as well as the load (or time) required for the specimen to failure above 5 wt%, resulted from the existence of weak links due to agglomerations in mechanical domain is correlated to the reduction in the decay rate as well as increment in trap energy states resulted from the formation of clusters of nanoparticles in the polymer matrix nearing the percolation threshold. Though the correlation between DIC and surface potential decay behaviour is found in the present study, further investigation is needed to validate this consistency for different filler material at various filler concentrations subjected to different mechanical and electrical loadings. Even though this correlation technique is at its infancy, viable predictions on electrical behaviour viz. threshold electric field, trap characteristics etc, can be made for other materials, if this consistency is validated.

4. Conclusions

The mechanical-electrical characteristics of Al/Epoxy nanocomposites were investigated with varying addition of Al nanoparticles. The performance of nano aluminium filler added epoxy nanocomposites was studied for the variation in surface strain and surface charge accumulation under mechanical and electrical stresses, respectively. The DIC technique was used to study the surface strain variation, while the needle plane configuration was employed to investigate the surface potential characteristics, to obtain the similarity in the surface properties in the electromechanical domain for different epoxy nano aluminium composites. The important conclusions drawn based on the present study are the following:

- The improvement in the load at maximum tensile stress and stiffness was noticed up to 5 wt% nanofiller addition, beyond which the depreciation was observed due to the microcracking initiated from the increased filler concentration.
- The variation in the surface strain and field displacement at different locations on the specimen loaded with different nanofiller concentrations were analysed through the DIC technique. It is clear from the results that the DIC method can detect the full-field shape, deformation, displacement and contour of strain measurements in the sample subjected to mechanical loading.
- The exponential decay in surface potential is observed irrespective of the magnitude and polarity of the applied voltage as well as with the filler content. Trap energy distribution covers in 0.7 eV to 0.9 eV for epoxy nano aluminium composites. A left shift in the trap depth is related to the increased decay rate.
- The optimized strain distribution resulted from the efficient stress transfer between the matrix and filler from DIC analysis corresponds to the existence of shallow energy states in providing the faster surface decay characteristics.
- The inefficient load transfer above 5 wt% measured through DIC is correlated with the reduction in the decay rate as well as an increment in trap energy states resulted from the formation of clusters of nanoparticles in the polymer matrix nearing the percolation threshold.

ORCID iDs

Naresh Chillu  <https://orcid.org/0000-0003-4024-9989>

R Jayaganthan  <https://orcid.org/0000-0002-3634-9306>

R Sarathi  <https://orcid.org/0000-0002-1353-9588>

References

- [1] Tanaka T and Imai T 2017 *Advanced Nanodielectrics: Fundamentals and Applications* 1st ed (New York: Jenny Stanford) (<https://doi.org/10.1201/9781315230740>)
- [2] Tanaka T 2005 Dielectric nanocomposites with insulating properties *IEEE Trans. Dielectr. Electr. Insul.* **12** 914–28
- [3] Mishra P, Desai B M A, Sarathi R and Imai T 2019 Performance analysis of epoxy nanocomposites due to water droplet-initiated discharges under AC and DC voltages and localisation of discharges *IET Sci. Meas. Technol.* **13** 175–85
- [4] Singha S and Thomas M J 2008 Dielectric properties of epoxy nanocomposites *IEEE Trans. Dielectr. Electr. Insul.* **15** 12–23
- [5] Wang Z, Zhou W, Sui X and Dong L 2015 Enhanced dielectric properties and thermal conductivity of Al/CNTs/PVDF ternary composites *J. Reinf. Plast. Compos.* **34** 1126–35
- [6] Paul S and Sindhu T K 2016 Effect of filler particle size on electric energy density of epoxy-aluminum nanocomposites *IEEE Trans. Dielectr. Electr. Insul.* **23** 2786–94
- [7] Usher M J and Keating D A 1996 Analogies between systems *Sensors and Transducers* (UK, London: Macmillan Education) pp 12–20
- [8] Olowojoba G B, Kopsidas S, Eslava S, Gutierrez E S, Kinloch A J, Mattevi C, Rocha V G and Taylor A C 2017 A facile way to produce epoxy nanocomposites having excellent thermal conductivity with low contents of reduced graphene oxide *J. Mater. Sci.* **52** 7323–44

- [9] Swain S, Sharma R A, Bhattacharya S and Chaudhary L 2013 Effects of nano-silica/nano-alumina on mechanical and physical properties of polyurethane composites and coatings *Trans. Electr. Electron. Mater.* **14** 1–8
- [10] Lim S H, Zeng K Y and He C B 2010 Morphology, tensile and fracture characteristics of epoxy-alumina nanocomposites *Mater. Sci. Eng. A* **527** 5670–6
- [11] Guo C, Zhou L and Lv J 2013 Effects of expandable graphite and modified ammonium polyphosphate on the flame-retardant and mechanical properties of wood flour-polypropylene composites *Polym. Polym. Compos.* **21** 449–56
- [12] Naresh C, Sarathi R, Rao B N, Danikas M, Tanaka T and Jayaganthan R 2019 Investigation on space charge and charge trap characteristics of Al-epoxy nanocomposites *IET Sci. Meas. Technol.* (<https://doi.org/10.1049/iet-smt.2019.0294>)
- [13] Nazarenko O B, Melnikova T V and Visakh P M 2016 Thermal and mechanical characteristics of polymer composites based on epoxy resin, aluminium nanopowders and boric acid *J. Phys. Conf. Ser.* **671** 012040
- [14] Fu Y-X, He Z-X, Mo D-C and Lu S-S 2014 Thermal conductivity enhancement with different fillers for epoxy resin adhesives *Appl. Therm. Eng.* **66** 493–8
- [15] Anithambigai P, Shanmugan S, Mutharasu D, Zahner T and Lacey D 2014 Study on thermal performance of high power LED employing aluminum filled epoxy composite as thermal interface material *Microelectronics J.* **45** 1726–33
- [16] Bello S, Agunsoye J, Adebisi J and Hassan S 2017 Effect of aluminium particles on mechanical and morphological properties of epoxy nanocomposites *Acta Period. Technol.* **48** 25–38
- [17] Naresh K, Shankar K, Rao B S and Velmurugan R 2016 Effect of high strain rate on glass/carbon/hybrid fiber reinforced epoxy laminated composites *Compos. Part B Eng.* **100** 125–35
- [18] Pan B 2018 Digital image correlation for surface deformation measurement: historical developments, recent advances and future goals *Meas. Sci. Technol.* **29** 082001
- [19] Du B X, Jiang J P, Zhang J G and Liu D S 2016 Dynamic behavior of surface charge on double-layer oil-paper insulation under pulse voltage *IEEE Trans. Dielectr. Electr. Insul.* **23** 2712–9
- [20] Saha D, Anisimov A G, Groves R M, Tsekmes I A, Morshuis P H F and Kochetov R 2017 Epoxy-hBN nanocomposites: A study on space charge behavior and effects upon material *IEEE Trans. Dielectr. Electr. Insul.* **24** 1718–25
- [21] Matsui K, Tanaka Y, Takada T, Fukao T, Fukunaga K, Maeno T and Alison J M 2005 Space charge behavior in low-density polyethylene at pre-breakdown *IEEE Trans. Dielectr. Electr. Insul.* **12** 406–15
- [22] Wang S, Luo S, Tu Y, Wang C and Qin S 2017 Effect of polarity reversal on space charge properties of CB/LDPE composite under DC field *IEEE Trans. Dielectr. Electr. Insul.* **24** 1349–54
- [23] Chen X, Wang X, Wu K, Peng Z R, Cheng Y H and Tu D M 2012 Effect of voltage reversal on space charge and transient field in LDPE films under temperature gradient *IEEE Trans. Dielectr. Electr. Insul.* **19** 140–9
- [24] Tanaka T, Kozako M, Fuse N and Ohki Y 2005 Proposal of a multi-core model for polymer nanocomposite dielectrics *IEEE Trans. Dielectr. Electr. Insul.* **12** 669–81
- [25] Paul S and Sindhu T 2014 Development of epoxy-aluminum nanocomposite dielectric material with low filler concentration for embedded capacitor applications *IEEE Trans. Dielectr. Electr. Insul.* **21** 460–6
- [26] Naresh C, Jayaganthan R, Danikas M G, Tanaka T and Sarathi R 2019 Understanding the dielectric and mechanical properties of self-passivated Al-epoxy nanocomposites *IET Sci. Meas. Technol.* **13** 1336–1344
- [27] Pan B, Qian K, Xie H and Asundi A 2009 Two-dimensional digital image correlation for in-plane displacement and strain measurement: a review *Meas. Sci. Technol.* **20** 062001
- [28] Moreira D C, Sphaier L A, Reis J M L and Nunes L C S 2012 Determination of Young's modulus in polyester-Al₂O₃ and epoxy-Al₂O₃ nanocomposites using the digital image correlation method *Compos. Part A Appl. Sci. Manuf.* **43** 304–9
- [29] Wang S, Li A, Xing Y, Li K and Li Z 2019 Surface potential and breakdown characteristics of epoxy/AlN nanocomposites under DC and pulse voltages *IEEE Trans. Appl. Supercond.* **29** 1–5
- [30] Du B X, Zhu W B, Li J, Xing Y Q and Huang P H 2017 Temperature-dependent surface charge behavior of polypropylene film under DC and pulse voltages *IEEE Trans. Dielectr. Electr. Insul.* **24** 774–83
- [31] Zakaria M R, Abdul Kudus M H, Akil H Md and Mohd Thirmizir M Z 2017 Comparative study of graphene nanoparticle and multiwall carbon nanotube filled epoxy nanocomposites based on mechanical, thermal and dielectric properties *Compos. Part B Eng.* **119** 57–66
- [32] Ab Ghani A F 2016 Digital image correlation technique in measuring deformation and failure of composite and adhesive *ARPJ. Eng. Appl. Sci.* **11** 13193–202
- [33] Li J, Zhou F, Min D, Li S and Xia R 2015 The energy distribution of trapped charges in polymers based on isothermal surface potential decay model *IEEE Trans. Dielectr. Electr. Insul.* **22** 1723–32
- [34] Molinie P 2005 Measuring and modeling transient insulator response to charging: the contribution of surface potential studies *IEEE Trans. Dielectr. Electr. Insul.* **12** 939–50
- [35] Du B X, Kong X X, Xing Y Q and Li J 2017 Trap distribution of electron beam irradiated epoxy resin under repetitive pulse voltage *IEEE Trans. Dielectr. Electr. Insul.* **24** 3869–77
- [36] Gao Y, Wang J, Liu F and Du B 2018 Surface potential decay of negative corona charged epoxy/Al₂O₃ nanocomposites degraded by 7.5-MeV electron beam *IEEE Trans. Plasma Sci.* **46** 2721–9